Proceedings World Geothermal Congress 2026
Calgary, Canada, June 8 – 11, 2026

Process Integration of Geothermal Energy with Solid Oxide Electrolysis for Low-Carbon Hydrogen Production

Romuald Coupan[1*], Joseph Wilding-Steele[1], Nicolas Valayé[1], Jati Permana Kurniawan[2], Mohamad Husni Mubarok[2]

GENVIA SAS, Plaine Saint Pierre, 34500 Béziers, France[1*],

PT Pertamina Geothermal Energy Tbk, 11-13 Jalan Medan Merdeka Timur, Jakarta Pusat 10110, Indonesia[2]

romuald.coupan@genvia.com RCoupan@slb.com

Keywords: Hydrogen, Electrolyzer, Geothermal Energy, Heat Recovery

ABSTRACT

High-temperature electrolysis using solid oxide electrolysis cells (SOEC) offers a promising pathway for producing low-carbon hydrogen from steam. This process benefits significantly from a continuous, carbon-free thermal energy source, making it particularly suitable for integration with geothermal energy. This study investigates the coupling of geothermal resources – in the form of hot brine or saturated steam – with a solid oxide electrolyzer (SOEL) system, analyzing both grid-connected and off-grid (standalone) configurations. A detailed process model is developed using a proprietary computational thermodynamic process modelling software. The integrated system includes geothermal heat extraction, a power generation unit based on a Steam Rankine Cycle (SRC) or Organic Rankine Cycle (ORC), and a heat recovery steam generator (HRSG) to meet the thermal requirements of the SOEL. Scenarios are modelled under varying geothermal conditions, energy conversion pathways, and operating modes. Two configurations are assessed: one in which geothermal heat is fed into the SOEL, with the latter drawing power from grid as needed; and another in which both geothermal electricity and heat are utilized locally for fully autonomous hydrogen production. The model evaluates overall system performance through heat and mass balances, electrical and thermal efficiencies, and CO_2 emissions reduction potential. The results demonstrate that geothermal-SOEL integration can enable efficient and sustainable hydrogen production, particularly in regions with accessible geothermal resources. Both quantitative and qualitative analyses highlight the key design parameters and trade-offs between energy efficiency, system autonomy, and carbon intensity. This study provides a foundation for the future deployment of decentralized, low-carbon hydrogen production systems powered by geothermal energy.

1 INTRODUCTION

According to the International Energy Agency, the decarbonization of energy systems requires both the rapid scale-up of renewable power generation and the development of low-carbon fuels for industry, transport, and seasonal storage (IEA, 2024). Hydrogen has emerged as a key energy carrier because it can be produced from water without direct CO_2 emissions and can serve as a feedstock or fuel in multiple sectors (IEA, 2025).

While alkaline electrolyzers (AEL) and proton exchange membrane electrolyzers (PEMEL) dominate the current market, and anion exchange membrane electrolyzers (AEMEL) emerge as a promising alternative, high-temperature electrolysis based on solid oxide electrolysis cells (SOEC) offers higher system efficiencies by utilizing heat in addition to electricity. When the necessary heat is supplied from a carbon-free source, solid oxide electrolyzers (SOEL) can achieve very low life-cycle greenhouse gas emissions compared to low-temperature electrolysis (Laurencin and Mougin, 2015).

Geothermal energy provides a uniquely suitable heat source for SOEL. It is baseload, renewable, and widely available in many regions of the world. Modern geothermal power plants already extract high-enthalpy fluids, generate electricity via steam or organic Rankine cycles, and return brine to the reservoir (Zarrouka and Moon, 2014). This infrastructure can be leveraged to supply both electricity and high-grade heat to an electrolyzer system without additional fossil-fuel combustion. Coupling geothermal and SOEL therefore has the potential to produce low-carbon hydrogen efficiently with near-zero emissions while also increasing the overall utilization of geothermal resources.

Despite this potential, few studies (Brillian et al., 2024) have quantified the technical performance of integrated geothermal-SOEC systems. Key questions remain on optimal process integration, such as the sharing of heat between power cycles and electrolysis, and the trade-offs between grid export and local consumption for

autonomous hydrogen production. In addition, modelling must account for varying geothermal temperatures, flow rates, and plant configurations.

This paper addresses these gaps by developing and analyzing a detailed process model of geothermal-SOEL integration. Using a proprietary thermodynamic modelling platform, we simulate both grid-connected and standalone configurations, including geothermal heat extraction, power generation, and heat-recovery steam generation. We evaluate heat and mass balances, electrical and thermal efficiencies, and the potential for CO_2 emission reductions under different resource and operating conditions. The objective is to identify the key design parameters and performance trade-offs that can inform the future deployment of decentralized, low-carbon hydrogen production systems powered by geothermal energy.

2 METHODOLOGY, PROCESS MODELLING, CALIBRATION, VALIDATION

This study is carried out using a detailed process modelling approach to evaluate the technical integration of geothermal resources with SOEL for low-carbon hydrogen production. The entire system, from geothermal fluid extraction to hydrogen generation, is represented using Symmetry®, the SLB proprietary thermodynamic process modelling software. The input parameters include the geothermal fluids characteristics, the fluid thermodynamic properties, the electrolyzer performances, and the overall system operating conditions.

2.1 Geothermal Resource Definition

The geothermal resource originates from eight production geothermal wells located in Ulubelu, Indonesia. Two-phase geothermal fluids extracted from the reservoir undergo initial treatment in separation units equipped with knockout drums, which divide the mixture into distinct gaseous and liquid streams. These geothermal fluids are characterized based on their mass enthalpy, pressure, mass flow rate, and chemical composition (Table 1).

Table 1. Steam and brine geothermal fluids characteristics from Ulubelu's wells.

	Steam				Brine			
Well	Flowrate (t/h)	Pressure (barg)	Temperature (°C)	Total NCGs (wt.%)	Flowrate (t/h)	Pressure (barg)	Temperature (°C)	Total dissolved solid (ppm)
N°1	21	9.5	178	0.6	84	7.6	178	2900
N°2	24	9.2	176	1.7	102	8.9	176	2720
N°3	71	6.6	163	0.5	121	5.6	163	2808
N°4	53	7.3	167	0.4	293	5.3	167	2446
N°5	21	8	170	0.2	118	7.7	170	2630
N°6	31	8.3	172	0.2	229	7.4	172	2412
N°7	72	8.6	173	0.9	157	5.2	173	2619
N°8	26	9.7	179	0.6	108	8.4	179	2782

The gaseous component of the geothermal fluid consists primarily of saturated steam, with less than 2 wt.% of non-condensable gases (NCG). These gases are composed of approximately 80–95% carbon dioxide, with the remainder including nitrogen, methane, hydrogen sulfide, hydrogen, ammonia, and argon. The liquid component is brine, with total dissolved solids (TDS) ranging from 2400 to 2900 ppm. It mainly contains solubilized sodium chloride, along with other dissolved minerals in ionic form such as potassium, calcium, carbonate, sulfate, and others.

2.2 Geothermal Energy Valorization Model

Two power conversion options are implemented in the model: a Steam Rankine Cycle (SRC) for steam resources and an Organic Rankine Cycle (ORC) for brine. Each power block is simulated solely for electricity generation.

Figure 1 illustrates the SRC, in which steam from the geothermal well is expanded to atmospheric pressure through a steam turbine operating at 85% adiabatic efficiency to produce electricity. The resulting low-pressure steam is then fully condensed using a cooling tower and subsequently reinjected into the well.

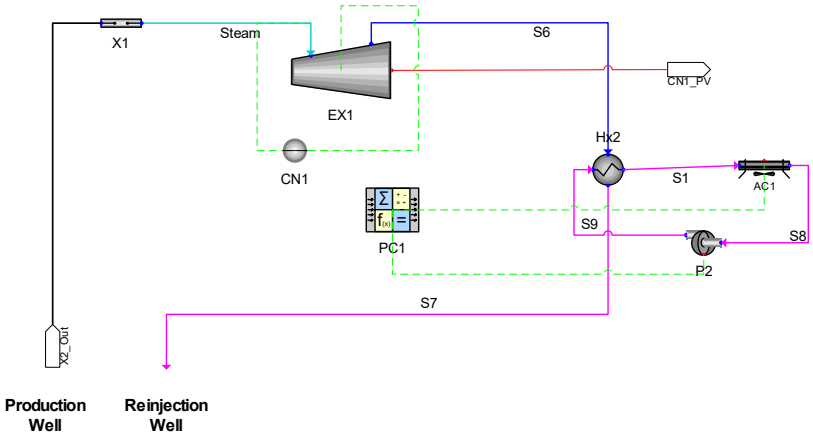


Figure 1. Sub-model of the Steam Rankine Cycle (SRC).

The ORC system, as presented in Figure 2, begins with brine from the geothermal well entering a heat exchanger, where it transfers heat to vaporize the circulating isopentane working fluid. The vaporized isopentane is expanded to atmospheric pressure through a turbine operating at 85% adiabatic efficiency, generating electricity. After expansion, the low-pressure isopentane is condensed using an air cooler, and the liquid is then pumped back to the heat exchanger to complete the cycle.

At the outlet of the heat exchanger, the cooled brine is reinjected into the well at a temperature between 120°C and 130°C. Maintaining this temperature range is essential to prevent mineral deposition and defines the threshold beyond which further heat extraction is not feasible.

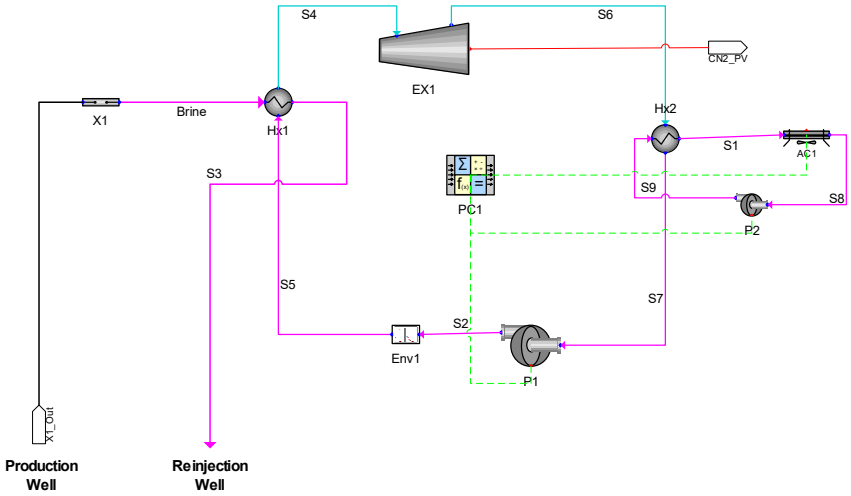


Figure 2. Sub-model of the Organic Rankine Cycle (ORC).

In addition to electricity production, the model also considers direct heat valorization options (see Figure 3) to utilize geothermal resources for generating superheated steam feedstock for SOEL. This latter is produced at suitable conditions (a minimum of 2.5 bara and 150°C) to meet the thermal requirements of the electrolyzer.

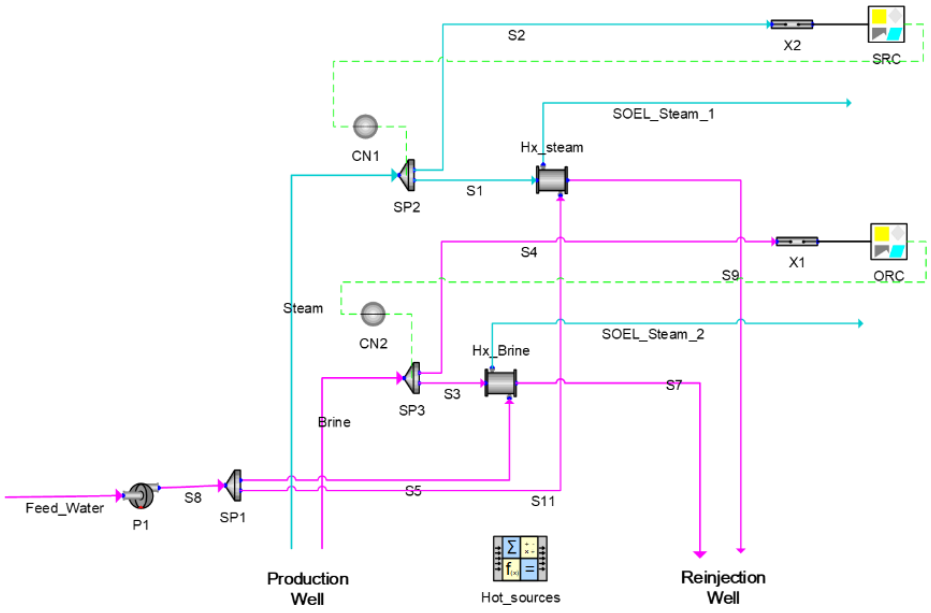


Figure 3. Sub-model of the Heat Recovery Steam Generator (HRSG).

A splitter enables full or partial redirection of either hot brine or saturated steam toward a Heat Recovery Steam Generator (HRSG). The HRSG is modeled as a typical thermal steam boiler, where geothermal fluid acts as the hot fluid, flowing in counter-current to the water/steam circuit. The HRSG is supplied with high-quality water from a water treatment unit located in the outside battery limits (OSBL) and is designed based on the temperature approach and reinjection temperature limits of 120 – 130°C for brine and approximately 30°C for steam.

2.3 SOEL Modelling and Assumptions

The SOEL is modelled as a high temperature electrolyzer fed with superheated steam (Coupan et al., 2025). Steam is introduced and mixed with recycled hydrogen to maintain a 10 mol.% hydrogen concentration at the system inlet, effectively preventing electrode oxidation. This mixture is heated to 800°C using a series of heat exchangers and an electric heater. In parallel, dry air used as sweep gas, is similarly heated. Both the hot steam and sweep gas enter the electrolysis cell stack, where oxygen is produced at the anode and removed by the sweep gas, resulting in 60 mol.% oxygen-enriched air. At the cathode, hydrogen is generated and exits with unreacted water, achieving a 70 mol.% water conversion rate. After cooling and water separation, part of the hydrogen stream is recycled to the inlet, while the remainder exits the SOEL unit at 1.4 bar with a purity of 98.5 mol.% hydrogen.

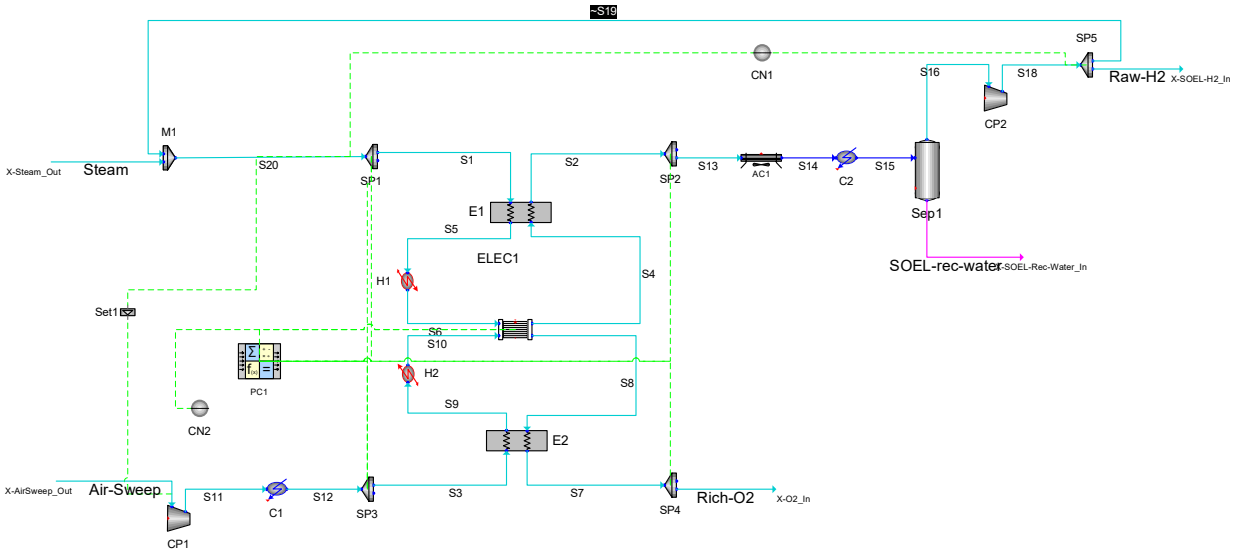


Figure 4. Sub-model of the SOEL high temperature electrolyzer (from [6]).

Electrical consumption and thermal requirements are defined based on current development-scale SOEL data: 39 kWh_e and 9 kW_{th} per kilogram of hydrogen. Heat recovery steam generator (HRSG) are added to transfer geothermal heat to the SOEL feedstock, minimizing the need for complementary electric heaters.

2.4 Configurations and Scenarios

Two integration configurations are developed: grid-connected and standalone modes. In the grid-connected mode, electricity for the SOEL unit is supplied from the grid, while geothermal heat is used to produce superheated steam feedstock. In the standalone mode, both electricity and heat are sourced directly from the geothermal resource, enabling fully autonomous hydrogen production on-site.

Several high-level scenarios, as presented in Table 2, are defined by combining the two integration modes with different valorization pathways – using geothermal saturated steam, hot brine, or both – to produce heat, power, or a combination of the two.

For each scenario, the model automatically resolved mass and energy balances to determine steam flow rates, electricity generation and consumption, heat recovery, and hydrogen output. Thermal and electrical efficiencies are calculated, along with the overall CO_2 emission reduction potential compared to conventional hydrogen production methods.

Table 2. High-level scenarios for geothermal energy valorization and hydrogen production.

		Geothermal Steam valorization		Hot Brine Valorization	
Scenario	Description	Heat to SOEL	Power to SOEL	Heat to SOEL	Power to SOEL
0	Grid-connected mode - Heat from steam + Heat from brine + External power source	Yes	No	Yes	No
0a	Grid-connected mode - Heat from steam + External power source	Yes	No	No	
0b	Grid-connected mode - Heat from brine + External power source	No		Yes	No
1	Stand-alone mode - Heat & Power from steam + Heat & Power from brine	Yes		Yes	
1a	Stand-alone mode - Heat & Power from steam	Yes		No	
1b	Stand-alone mode - Heat & Power from brine	No		Yes	
2	Stand-alone mode - Heat from brine + Power from steam	No	Yes	Yes	No
3	Stand-alone mode - Heat & Power from brine + Power from steam	No	Yes	Yes	

3 RESULTS AND DISCUSSION

The simulation results reveal that hydrogen production yield varies significantly depending on the integration configuration and the pathway used to valorize geothermal resources. Since the SOEL unit operates at a fixed efficiency – requiring 39 kWh_e and 9 kWh_{th} per kilogram of hydrogen – the overall system performance is governed by the availability and quality of electricity and heat rather than changes in electrolyzer efficiency.

The analysis – based on calculations across the eight varying well conditions – shows that hydrogen yield and system efficiency are highly dependent on geothermal fluid temperature and flow rate. A 10°C increase in steam temperature improves hydrogen output by 8–12%, due to increased enthalpy. Similarly, any increase in flow rate enhances power generation and heat recovery. Conversely, lower enthalpy resources require more auxiliary heating and reduce overall efficiency.

In the grid-connected configuration (see Figure 5), where electricity is supplied externally and geothermal heat is used solely for SOEL steam feedstock generation, the system achieves a hydrogen production yield per well ranging from 1.7–6.0 t/h for geothermal steam sources (scenario 0a) and 0.9–2.5 t/h for hot brine sources (scenario 0b). These figures are based on total grid electricity inputs of 68–234 MW_e and 20–54 MW_e for geothermal steam and brine, respectively. The corresponding thermal energy demands are 16–54 MW_{th} and 5–14 MW_{th}. Saturated steam from geothermal wells provides more enthalpy, enabling greater hydrogen production due to its high energy content of approximately 2790 kJ/kg, compared to brine, which ranges between 1100 and 1300 kJ/kg.

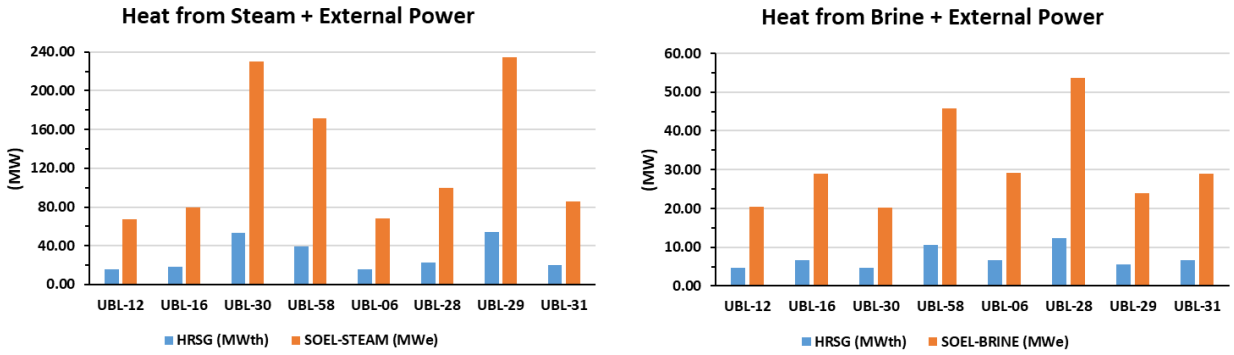


Figure 5. Geothermal resource valorization for SOEL coupling in an external power grid-connected mode (scenarios 0a and 0b).

In contrast, as shown in Figure 6, the standalone configuration – relying entirely on geothermal resources for both electricity and heat – shows lower hydrogen yields due to limited power generation capacity. For example, with only 2.3–8.1 MW_e of geothermal electricity available from steam sources (scenario 1a), the SOEL unit produces just 60–210 kg/h of hydrogen, with a thermal demand of 0.5–1.9 MW_{th}. From geothermal brine sources (scenario 1b), yields range from 23–61 kg/h, corresponding to SOEL unit sizes of 0.9–2.4 MW_e and thermal demands of 0.2–0.6 MW_{th}. In heat and power mode, about 96–97% of the heat source is used for electricity production in both SRC and ORC, while the remaining 3–4% is used for SOEL steam feedstock production in the HRSG.

Standalone heat and power mode produces approximately 92–96% less hydrogen than the grid-connected mode. Despite the lower throughput, this configuration offers complete energy independence.

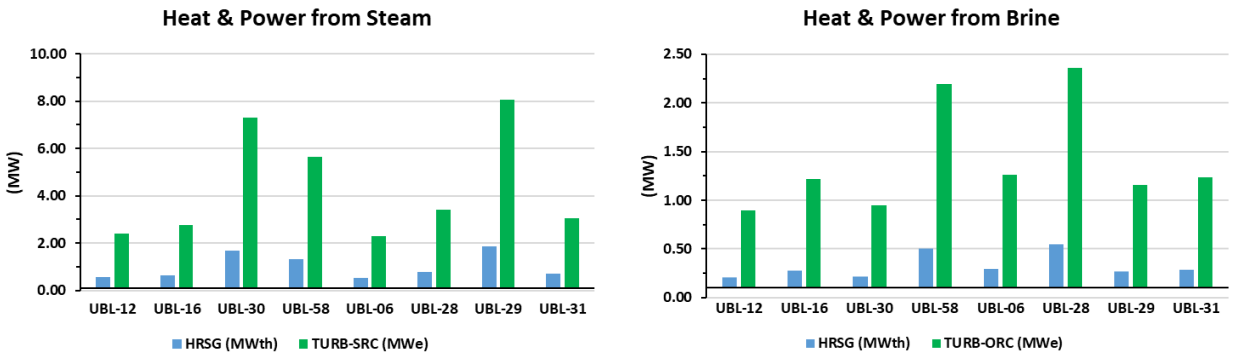


Figure 6. Geothermal resource valorization for SOEL coupling in a standalone heat & power mode (scenarios 1a and 1b).

By combining the heat and power capabilities of both geothermal steam and brine, the global configuration (Scenario 1) serves as a performance benchmark for evaluating alternative standalone setups. In this scenario, steam and brine are jointly valorized to maximize electricity generation and thermal input for SOEL operation, enabling the highest hydrogen yield through the synergistic use of high-enthalpy steam and hot brine. Scenario 2 presents a more constrained configuration, where electricity is generated solely from steam via the SRC, and the amount of heat extracted from brine is determined by the thermal demand of the SOEL unit, which is itself limited by the SRC's electricity output. This setup restricts hydrogen production due to reduced energy flexibility and lower overall resource utilization. Scenario 3 adopts a more integrated approach, combining steam-based power generation with both heat and power recovery from brine. This dual valorization improves system

performance and closely approaches the hydrogen output of Scenario 1, although with slightly reduced electricity generation capacity due to resource partitioning. The comparative analysis of these configurations underscores the critical role of multi-resource integration in optimizing hydrogen production under standalone conditions, particularly where external electricity supply is unavailable.

Hydrogen production rates across all three standalone scenarios (see Figure 7) range from 60 to 240 kg/h. The highest yield of 240 kg/h (SOEL size of 9.2 MW_e) is observed in scenario 1. In scenario 2, the yield reaches around 210 kg/h based on an 8.3 MW_e input. The lowest yield of 60 kg/h also occurs in this latter case, constrained by the 2.5 MW_e geothermal electricity limit. Scenario 3 is found to be very close (about 0.1 MW_e less electricity production) to scenario 1.

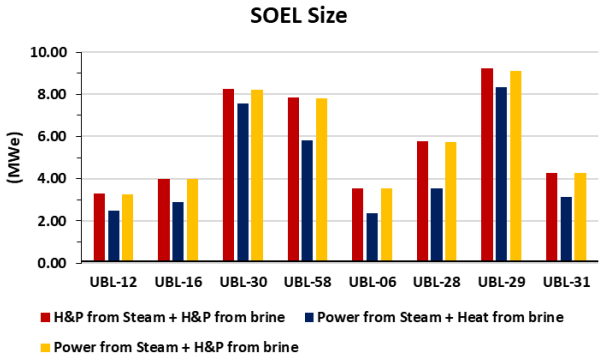


Figure 7. Geothermal resource valorization for SOEL coupling in a standalone mode (scenarios 1, 2 and 3).

Direct CO_2 emissions are also evaluated based on geothermal fluid composition, assuming no CO_2 reinjection, and the carbon footprint of the electric grid. Reference carbon emissions for hydrogen production via steam methane reforming (SMR) are estimated at 11.2 kg CO_2 equivalent per kg of hydrogen produced (Hyunah Cho et al., 2022; Coupan et al., 2025). This includes 9.35 kg of direct emissions and 1.87 kg from upstream processes.

For grid-connected scenarios, the carbon footprint of hydrogen production depends on both the grid's carbon intensity and direct emissions from wells. Assuming Indonesia's electricity generation carbon intensity of 682 g CO_2 per kWh_e (Our World in Data, 2024), the hydrogen produced has a footprint of 27 kg CO_2 equivalent per kg – more than double the SMR reference. However, using a low-carbon electricity mix such as France's (44 g CO_2 per kWh_e (Our World in Data, 2024)), emissions can be reduced by 83–85%, resulting in a footprint of about 1.8 kg CO_2 equivalent per kg of hydrogen.

In contrast, for standalone systems, only emissions from wells are considered. Hydrogen produced in these configurations has a footprint ranging from 0.3 to 5.1 kg CO_2 equivalent per kg, depending on well emissions and the energy valorization pathway. Geothermal electricity in these cases shows a carbon intensity between 9 and 132 g CO_2 per kWh_e.

4 CONCLUSION AND PERSPECTIVES

This study demonstrates the technical feasibility and environmental advantages of integrating solid oxide electrolyzer (SOEL) with geothermal energy for decentralized, low-carbon hydrogen production. Through detailed thermodynamic modeling of both grid-connected and standalone configurations, we show that hydrogen yield is highly sensitive to geothermal fluid temperature, flow rate, and the chosen valorization pathway.

Grid-connected systems offer higher throughput but rely on external electricity sources, whereas standalone configurations provide energy independence with significantly lower carbon footprints. The results highlight that geothermal steam, due to its higher enthalpy, enables greater hydrogen output compared to brine. However, combining steam and brine resources in hybrid scenarios can optimize both heat and power utilization, enhancing system flexibility.

Importantly, the carbon intensity of hydrogen produced from geothermal-SOEL systems ranges from 0.3 to 5.1 kg CO_2 per kg H_2 in standalone mode – substantially lower than conventional steam methane reforming (SMR) and even outperforming low-carbon grid-connected alternatives under favorable conditions.

These findings underscore the potential of geothermal-SOEL integration as a scalable pathway for low-carbon hydrogen production, especially in regions with abundant geothermal resources.

Although outside the scope of this study, preliminary estimates suggest that hydrogen production costs could reach 1.9 to 5.6 € per kg under favorable geothermal conditions, depending on system configuration and electricity sourcing. Operational flexibility and grid services could further improve project economics.

Future work should extend this modelling to techno-economic assessment, lifecycle analysis, transportation and pilot-scale demonstration to validate performance under real operating conditions. Additional studies on operational flexibility, seasonal resource variability, and integration with local hydrogen demand or storage could further strengthen the case for deploying decentralized, low-carbon hydrogen production systems powered by geothermal energy. By leveraging existing geothermal infrastructure, this approach can accelerate the transition toward sustainable energy systems and contribute meaningfully to global decarbonization goals.

Acknowledgements

The authors would like to acknowledge the project members, supporters, and facilitators from *PT Pertamina Geothermal Energy Tbk* and *PT Pertamina New & Renewable Energy*, and in particular Muhammad Taufik, Ramaditio Bagus Pradana, and Candra Sri Sutama.

REFERENCES

Brilian V. A., Akbar F. M., Majid A. I., Khasani, Mubarok M. H.: Preliminary Study of Integrated Bottoming Binary Cycle and Electrolysis Unit to Utilize Separated Brine at Ulubelu Geothermal Power Plant for Green Hydrogen Production, *AIP Conference Proceedings*, THERMOFLUID XII: The 12th International Conference on Thermofluids, Yogyakarta, Indonesia (2024).

Coupan R., Karam K., Al-Yaarubi A.: Insight in the Decarbonization of Oil Refining by Integrating High-Temperature Electrolysis, SPE Conference at Oman Petroleum & Energy Show, Muscat, Oman (2025).

Hyunah Cho H., Strezov V., Evans T. J., Environmental Impact Assessment of Hydrogen Production via Steam Methane Reforming Based on Emissions Data, *Energy Reports*, **8**, (2022), 13585 – 13595.

International Energy Agency, Renewables 2024, IEA, Paris, (2024). https://www.iea.org/reports/renewables-2024

International Energy Agency, Global Hydrogen Review 2025, IEA, Paris (2025). https://www.iea.org/reports/global-hydrogen-review-2025

Laurencin J., Mougin J., High-Temperature Steam Electrolysis, Hydrogen Production: Electrolysis, Agata Godula-Jopek (Ed.), Wiley-VCH Verlag GmbH & Co, (2015), 191 – 272.

Our World in Data. Carbon intensity of electricity generation (2024). https://ourworldindata.org/grapher/carbon-intensity-electricity

Zarrouka S. J., Moon H.: Efficiency of geothermal power plants: A Worldwide Review, *Geothermics*, **51**, (2014), 142 – 153.